

Received: 2019.02.19
Accepted: 2019.04.25
Published: 2019.08.15

Plumbagin Restrains Hepatocellular Carcinoma Angiogenesis by Stromal Cell-Derived Factor (SDF-1)/CXCR4-CXCR7 Axis

Authors' Contribution:

Study Design A
Data Collection B
Statistical Analysis C
Data Interpretation D
Manuscript Preparation E
Literature Search F
Funds Collection G

BC 1 **Jing Zhong***
FG 1 **Junxuan Li***
CD 1 **Jiexiao Wei***
CF 1 **Delun Huang**
AG 2 **Lini Huo**
DE 1 **Chuan Zhao**
BC 1 **Yuning Lin**
CD 1 **Wanjun Chen**
AEG 1 **Yanfei Wei**

1 Department of Physiology, Faculty of Basic Medicine, Guangxi University of Chinese Medicine, Nanning, Guangxi, P.R. China
2 Department of Organic Chemistry, Faculty of Pharmacy, Guangxi University of Chinese Medicine, Nanning, Guangxi, P.R. China

* Jing Zhong, Junxuan Li and Jiexiao Wei equal contributors

Corresponding Author: Yanfei Wei, e-mail: weiyangfei@gxcmu.edu.cn

Source of support: This project was supported by grants from the National Natural Science Foundation of China (81760757, 81260675, and 81560690); the Youth Innovation Team of Guangxi University of Traditional Chinese Medicine, Grant/Award Number (2015QT001); the Hundred Talents Plan for the Introduction of High-Level Overseas Talents by Guangxi Colleges and Universities, and the Guangxi Key Laboratory of Translational Medicine for Treating High-Incidence Infectious Diseases with Integrative Medicine

Background: Anti-angiogenic therapy has recently emerged as a highly promising therapeutic strategy for treating hepatocellular carcinoma (HCC).


Material/Methods: We assessed cellular proliferation, invasion, and activation of growth factors (VEGF and IL-8) with SDF-1 induced in the hepatocellular carcinoma cell line SMMC-7721, and this progression was limited by plumbagin (PL). The human umbilical vein endothelial cell line HUVEC was co-cultured with SDF-1-induced SMMC-7721, and the expressions of CXCR7, CXCR4, and PI3K/Akt pathways after PL treatment were detected by RT-PCR and Western blot analysis.

Results: The treatment of the hepatoma cell line SMMC-7721 with SDF-1 resulted in enhanced secretion of the angiogenic factors, IL-8 and VEGF, and shows that these stimulatory effects are abolished by PL. The study further demonstrated that PL not only abolishes SDF-1-induced formation of endothelial tubes, but also inhibits expression of CXCR4 and CXCR7, and partially prevents activation of angiogenic signaling pathways.

Conclusions: The effect of PL on the SDF-1-CXCR4/CXCR7 axis has become an attractive target for inhibiting angiogenesis in hepatoma cells. Our results provide more evidence for the clinical application of PL as part of traditional Chinese medicine in modern cancer treatment.

MeSH Keywords: **Angiogenesis Inducing Agents • Carcinoma, Hepatocellular • Chemokine CXCL12 • Plumbaginaceae • Receptors, CXCR4**

Full-text PDF: <https://www.medscimonit.com/abstract/index/idArt/915782>

 3265

 1

 5

 34



Background

Globally, hepatocellular carcinoma (HCC) is one of the most common malignancies and it accounts for 50.5% of Chinese cancer cases [1]. Forming new vessels or establishment of an abnormal angioarchitecture is a prerequisite for tumor growth [2]. Chemokines are crucial determinants of pathogenesis and outcome of hepatic disease. Furthermore, the tumor itself influences these cells to create a background that promotes stromal cells overexpression of CXCR4 and CXCR7, which are not just active bystanders, but play a substantial and active role in diverse tumor processes, including migration, invasion, growth, and angiogenesis [3]. Therefore, studying the molecular mechanism of chemokines in the angiogenesis, migration and growth of liver cancer tumors is of great importance in improving the immune microenvironment, extracellular matrix, and angiogenesis.

Plumbagin (5-hydroxy-2-methyl-1,4-naphthoquinone, PL), a naturally occurring naphthoquinone widely distributed in the Plumbaginaceae family, has been reported to possess a wide spectrum of biological and pharmacological properties, including activities against virus, bacteria, and various cancers [4]. Recent pharmacological studies have shown that PL serum can significantly inhibit proliferation of hepatic stellate cells and induce apoptosis. The mechanism involved may be arrest of its cycle in the G0/G1 phase and preventing it from passing the G1/S checkpoint [5]. In addition, PL promotes activation of activated hepatic stellate cells, upregulates the expression of P53 and Bax proteins in activated HSC, downregulates the expression of Bcl-2 protein, and induces production of cyclin-dependent protein kinase inhibitor (CD KI)-P21. In addition, it regulates cell cycle arrest in S-G2/M phase [6]. In HCC, PL upregulates the expression of p21, inhibits the proliferation, invasion, and expression of MMP-2 and MMP-9 in SKhep human hepatoma cells [7], and increases the ratio of Bax/Bcl-2 in hepatoma cells. It also downregulates the transcription level of Cyclin D1, reducing cell proliferation activity [8]. In addition, PL inhibits the invasion and migration of breast and gastric cancer cells by downregulating the expression of the chemokine receptor CXCR4 [9]. Our previous study demonstrated that PL treatment significantly suppressed tumor angiogenesis in cells and limited xenograft tumor growth, mostly by the related signaling pathways (PI3K-Akt, VEGF/KDR and Angiopoietins/Tie2) [10]. PL can also affect the autophagy and apoptosis of hepatocellular carcinoma SMMC-7721 cells [11].

To identify whether PL inhibits tumor-derived vascular endothelial cells via the SDF-1/CXCR4-CXCR7 axis, the present study evaluated the anticancer potential of PL *in vitro*, and further validated the hepatoma angiogenesis and mechanism initiated by PL, providing more evidence supporting PL as an alternative treatment of HCC.

Material and Methods

Cell proliferation assay

SMMC-7721 (KeyGen Biotech Co., Nanjing, China) and HUVEC (American Type Culture Collection, VA, USA) cells were cultured in high-glucose DMEM (Vazyme Biotech Co., Nanjing, China) supplemented with 10% fetal bovine serum FBS (Vazyme) in a humidified atmosphere containing 5% CO₂. Cells in the exponential phase were harvested at approximately 80% confluence. The SMMC-7721 cells were plated at a density of 5×10³ cells/well in 96-well plates. After 24 h of culture, the SMMC-7721 cells were exposed to various concentrations of SDF-1 (Sigma, St Louis, MO) (0, 1, 10, or 100 ng/ml) for 12, 24, or 48 h. Then, SMMC-7721 cells were exposed to various concentrations of PL (1.25, 2.5, 5.0, 7.5, or 10 μM) for 12, 24, or 48 h. These levels were measured using the CCK-8 assay (Vazyme, Nanjing, China).

Co-culture of HUVEC cells with SMMC-7721 cells

The cell culture medium consisted of DMEM+10% FBS+1% (penicillin–streptomycin solution)/1640+10% FBS+1% (penicillin–streptomycin solution). SMMC-7721 cells in logarithmic growth phase were grown to confluence. We inoculated 2×10⁵ cells per well into 6-well plates, with a total of 18 wells, and cultured them overnight in a 37°C 5% CO₂ incubator. The serum medium was further treated with SMMC-7721 cells for 24 h and replaced with normal DMEM medium and different concentrations of PL- or AMD3100 (Sigma, St Louis, MO)-treated SMMC-7721 cells. We took HUVEC cells in logarithmic growth phase and inoculated them into 21 wells in the lower layer of Transwell 6-well plates with 2×10⁵ cells per well, and cultured them overnight in a 7°C 5% CO₂ incubator. SMMC-7721 cells were seeded in the upper layer of the Transwell chamber. The final concentrations of PL in the medium were 2.5 μmol/L, 5.0 μmol/L, and 7.5 μmol/L. The final concentration of SDF-1 was 10 ng/ml, and the final concentration of AMD3100 was 100 ng/ml. After 24 h of treatment, the cells were photographed and the lower layer of endothelial cells were collected for assessment.

Transwell migration assay and enzyme-linked immunosorbent assay (ELISA)

A total of 5×10⁵ SMMC-7721 cells (200 μL) were added to the upper chambers of Transwell inserts with 8-μm pores in 24-well plates (Corning, CA, USA). Migration was induced by SDF-1 (PeproTech, NJ, USA) with 10% FBS-supplemented medium added to the lower chambers. Next, serum-free medium containing various concentrations of PL (1.25, 2.5, 5.0, 7.5, or 10 μM) was added, and the cells were pretreated for 48 h in 24-well plates. Then, non-adherent cells in the chambers were

Table 1. RT-PCR primers.

Name	Primer	Sequence
homo β -actin	Forward	5'-AGCGAGCATCCCCAAAGTT-3'
	Reverse	5'-GGGCACGAAGGCTCATCATT-3'
homo CXCR4	Forward	5'-CGTCCACGCCACCAACAGTCAGA-3'
	Reverse	5'-CCAGGCAGGATAAGGCCAACCAT-3'
homo CXCR7	Forward	5'-TGCTGCGTCAACCTGTCTCTA-3'
	Reverse	5'-CGATGAGCTTGGTGAGCCCTGTT-3'

removed and the inserts were fixed in 4% paraformaldehyde and stained with 2.5% crystal violet. Numbers of migrated cells were counted in 5 different fields under an inverted microscope (Leica, MK, UK). The vascular endothelial growth factor (VEGF) and interleukin-8 (IL-8) concentrations in cell supernatant were measured using ELISA kits (Boster, Wuhan, China).

Real-time polymerase chain reaction analysis

Total RNA of liver tissue samples was isolated using TRIzol reagent (TianGen Biotech Co., Beijing) according to the manufacturer's instructions. The concentration and the purity were measured using a Nanodrop 2000 spectrophotometer (Thermo Fisher Scientific, America). A RevertAid™ First-Strand cDNA Synthesis Kit (Fermentas) was used to synthesize cDNA using a PTC-220 multi-channel PCR (MJ, USA) according to the manufacturer's directions. The reverse transcription products were stored at 70°C for further use. The primers were synthesized by Shanghai Sangon Biological Engineering Co. (Shanghai, China) and are listed in Table 1. Afterward, RT-PCR was performed by fixing 10 μ l Dream TaqTMGreen PCR Master Mix (2 \times) (Fermentas), 0.5 μ l Forward primer, 0.5 μ l Reverse primer, 1 μ l cDNA samples, and 13 μ l water. All steps were performed according to the manufacturer's instructions. The semi-quantitative PCR products were identified by electrophoresis in 2.0% agarose gel (100 V, 30 min). The PCR signal intensities were detected by scanning the agarose gel with a gel imaging analyzer (Bio-Rad, USA) after electrophoresis.

Western blot analysis

Each group of cells was collected in the logarithmic growth phase, collecting 5–10 \times 10⁶ cell/ml cells. Cells were washed twice with cold PBS, 500 μ l cold lysate was added, and after mixing, were shaken at 4°C for 15–20 min, and then centrifuged at 16 000 g at 4°C for 15 min. Protein concentration was measured by the BCA method of the supernatant. We added 4 \times SDS sample treatment solution, and the samples were subjected to 100°C heating for 5 min of denaturation. After SDS-PAGE electrophoresis, protein was transferred from SDS polyacrylamide gels to nitrocellulose (PVDF) membranes. After the

transfer was completed, PVDF membranes were blocked for 1 h in 5% nonfat dry milk in TBST buffer at room temperature. The appropriate dilutions of primary antibodies were added as follows: anti- β -actin (1: 1000, Abcam Cambridge, MA, USA), CXCR4 (1: 1000, Abcam Cambridge, MA, USA), Akt (1: 1000, Abcam Cambridge, MA, USA), PI3K (1: 1000, Abcam Cambridge, MA, USA), CXCR7 (1: 1000, Sigma St Louis, MO, USA), p-PI3K (1: 1000, Santa Cruz, CA, USA), and p-Akt (1: 1000, Santa Cruz, CA, USA), and then incubated overnight at 4°C. Suitable secondary antibodies – HRP-labeled goat anti-mouse IgG antibody (1: 12 000) and HRP-labeled goat anti-rabbit IgG antibody (1: 10 000) – were then added and incubated at room temperature for 1 h. The ECL chemiluminescence method was utilized. We performed X-ray film exposure, development of chemiluminescence, and film scanning, and quantitative analysis was conducted using ImageJ software (US NIH). Anti- β -actin antibody was used as an internal loading control. The results are derived from the gray-value ratio of the target band and internal loading control.

Statistical analysis

Statistical analysis was performed using SPSS 22.0 (Chicago, IL, USA). Comparisons between 2 groups were made using ANOVA, and each mean pairwise comparison was analyzed using the q test.

Results

Effect on proliferation, migration, and expression of the angiogenesis indicators VEGF/IL-8 of SMMC-7721 cells induced by SDF-1

Different concentrations (0 ng/ml, 1 ng/ml, 10 ng/ml, and 100 ng/ml) of SDF-1 were used at different times (12 h, 24 h, 48 h). CCK-8 analysis showed that, in addition to the control group, the proliferation of SMMC-7721 cells was concentration-dependent after SDF-1 induced 3 doses of 1 ng/ml, 10 ng/ml, and 100 ng/ml, and the most obvious was at 24 h. At 48 h, there was no significant difference between the 3 concentrations and

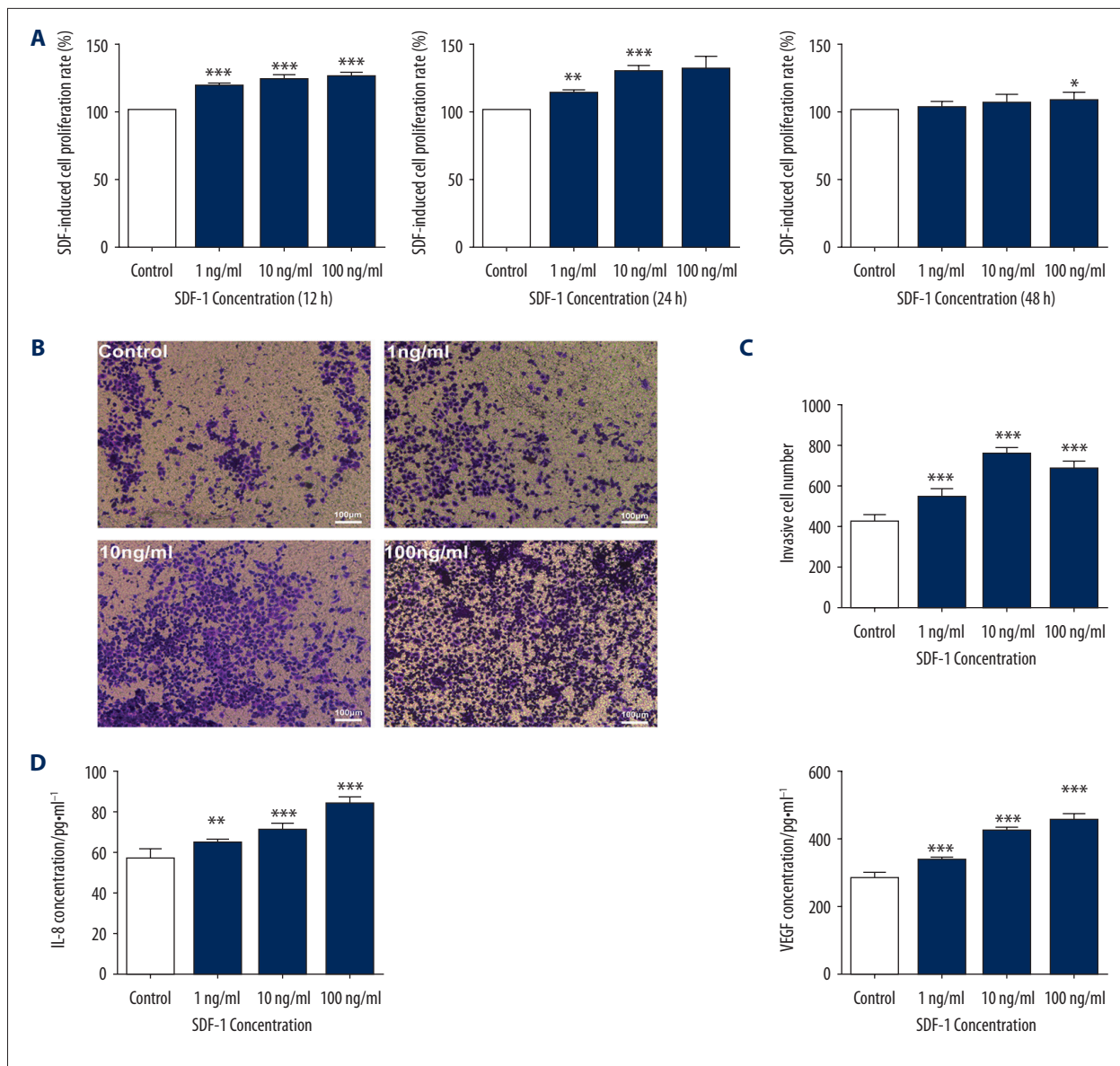


Figure 1. Proliferation of SMMC-7721 cells treated with various concentrations of SDF-1 (1 ng/ml, 10 ng/ml, and 100 ng/ml) for 12 h, 24 h, or 48 h in a 5% CO₂ incubator at 37°C. Each bar represents the mean value ± standard deviation (SD), * P<0.05; ** P<0.01; *** P<0.001, compared to the Control group (A). Microscopy of invasion of SMMC-7721 cells by different concentrations of SDF-1 (1 ng/ml, 10 ng/ml, and 100 ng/ml) (scale bar, 100 µm) (B). Numbers of invasive SMMC-7721 cells induced by different concentrations of SDF-1 (1 ng/ml, 10 ng/ml, and 100 ng/ml) (C). Effects of different concentrations of SDF-1 (1 ng/ml, 10 ng/ml, and 100 ng/ml) on secretion of IL-8 and VEGF in SMMC-7721 cells. Each bar represents the mean value ± standard deviation (SD), * P<0.05; ** P<0.01; *** P<0.001, compared to the Control group (D).

the control group, indicating that SDF-1 had no time-dependent effect on the proliferation of SMMC-7721 cells (Figure 1A). Transwell analysis showed that the invasive ability was the most obvious with the 10 ng/ml SDF-1 intervention for 24 h (P<0.01). The results of comprehensive cell proliferation assay and cell invasion assay showed that SDF-1 induced SMMC-7721 cells to construct an angiogenic microenvironment at a concentration of 10 ng/ml and the optimal intervention time

was 24 h (Figure 1B, 1C). The SMMC-7721 cell angiogenesis model was induced by different concentrations of SDF-1. The results showed that the levels of the 2 factors showed a certain dependence with the increase of SDF-1 concentration and were statistically significant (** P<0.01) (Figure 1D).

Effect of PL on proliferation, migration, and expression of angiogenesis indicators VEGF/IL-8 of SMMC-7721 cells were induced by SDF-1

Compared with the control group, SMMC-7721 was induced by SDF-1 to construct a hepatocellular angiogenesis microenvironment model, and the proliferation and invasion abilities of the model were enhanced. However, after intervention with different concentrations of PL, the proliferation inhibition ability of PL decreased gradually after 24 h. At 24 h, the efficacy of PL was the highest, and the proliferation of hepatoma cells was inhibited ($P < 0.01$ or $P < 0.05$). There was no significant difference in the proliferation rate of each concentration group at 48 h, indicating that PL had no time-dependent inhibition of proliferation of SMMC-7721 cells. AMD3100 was used as a positive control group, as shown in Figure 2A. In addition, in the absence of SDF-1, PL has the ability to inhibit proliferation of SMMC-7721 cells. At the 48-h timepoint, the value-added rate of PL alone was lower than that of SDF-1 and PL, indicating that SDF-1 has an antagonistic effect on PL-inhibited proliferation of SMMC-7721 cells (Figure 2B). The invasive ability of hepatoma cells after treatment with PL was gradually decreased, showing a certain concentration dependence, as shown in Figure 2C, 2D. The results of the 2-part analysis showed that the proliferation inhibition ability and invasive ability of the 3 groups of concentration gradients (2.5 $\mu\text{mol/ml}$, 5.0 $\mu\text{mol/ml}$, and 7.5 $\mu\text{mol/ml}$) were more obvious. The secretion of VEGF and IL-8 by PL had a certain concentration-dependent effect. The 5 concentrations have obvious inhibitory effects on VEGF ($P < 0.01$), and the secretion of IL-8 was significant. The inhibitory effect was most obvious with the first 4 concentrations. When the concentration of PL dandelion reached 7.5 $\mu\text{mol/ml}$ and above, the effect of inhibiting VEGF was equivalent to that of AMD3100. When the concentration of PL reached 5.0 $\mu\text{mol/ml}$ and above, the effect of inhibiting IL-8 was the same. The AMD3100 was basically the same, as shown in Figure 2E.

Effects of PL on the angiogenesis co-culture model of HCC and the expression of angiogenesis markers CXCR4 and CXCR7 mRNA

Overexpression of CXCR4 and CXCR7 can induce angiogenic capacity and tumor growth [12,13]. CXCR4 is the only high-affinity receptor for SDF-1, and it was demonstrated to be involved in development, progression, metastasis, and epithelial-mesenchymal transition [14]. Another receptor, CXCR7, mediated a broad range of cellular activities, including adhesion, invasion, VEGF production, and angiogenesis, by binding with SDF-1 [15]. The results showed that CXCR4 and CXCR7 mRNA were expressed at a low level in HUVEC human umbilical vein endothelial cells. When co-cultured with HUVEC human umbilical vein endothelial cells, mRNA expression levels of both receptors increased, among which CXCR7 mRNA expression

of CXCR4 mRNA was significantly higher than that of CXCR7 mRNA ($P < 0.01$). The expression of CXCR7 and CXCR4 mRNA was significantly increased by induction of SDF-1 ($P < 0.01$). The inhibition of CXCR7 mRNA was significantly inhibited by 2.5 $\mu\text{mol/ml}$ PL ($P < 0.05$) and the inhibition of CXCR4 mRNA required 5.0 $\mu\text{mol/ml}$ PL to play a significant role ($P < 0.05$). When the PL concentration reached 5.0 $\mu\text{mol/ml}$ and above, the mRNA of CXCR4 and CXCR7 expression was significantly decreased ($P < 0.01$), and the inhibition rates were 22.03% and 17.03%, respectively. Figure 3A shows that PL can down-regulate the mRNA expression levels of CXCR4 and CXCR7.

SMMC-7721 human hepatoma cells were induced by SDF-1 and directly co-cultured with HUVEC human umbilical vein endothelial cells. Normal HUVEC cells were distributed in a lumen-like manner on Matrigel gel, forming a blood vessel-like structure, but with a small number of lumens. The diameter of the cells in the co-culture group was multi-tubular-like and the diameter of the lumen was large. Our results show that secretion of related factors in SMMC-7721 cells enhanced the angiogenic ability of HUVEC cells. When SDF-1 was induced, the tubule-like structure formed by HUVEC increased significantly. The lumen was larger; when the antagonist AMD3100 was added, the distribution of vascular endothelial cells was disordered, and there was no tubule-like structure. The angiogenesis was significantly reduced with increased concentration (Figure 3B).

PL upregulates phosphorylation levels of PI3K/Akt and affects SDF-1/CXCR4 and SDF-1/CXCR7 signaling pathways

We further explored whether PL can inhibit SDF-1 induced by co-culture of HUVEC cells with SMMC-7721 cells by blocking of the PI3K/Akt, SDF-1/CXCR4, and SDF-1/CXCR7 signaling pathways in HUVEC cells. Compared with the single-culture HUVEC human umbilical vein endothelial cells group and SDF-1 group, Akt phosphorylation was significantly decreased by medium and higher doses. In the AMD3100 group (** $P < 0.01$), the concentration was high and the phosphorylation level of PI3K was significantly decreased by AMD3100 antagonism (** $P < 0.01$). There was no difference in the total protein levels of Akt and PI3K in each treatment group ($P > 0.05$) (Figure 4A, 4B). These results indicate that CXCR4 and CXCR7 may be tightly associated with the levels of angiogenesis-related proteins ($P < 0.01$), and CXCR7 plays an essential role. Moreover, the overexpression of PI3K-Akt, CXCR4, and CXCR7 was significantly suppressed in a dose-dependent manner ($P < 0.01$) by PL treatment *in vitro*.

Discussion

The main purpose of this study was to assess whether PL can abolish SDF-1/CXCR4-CXCR7 activation of the PI3K/Akt pathway

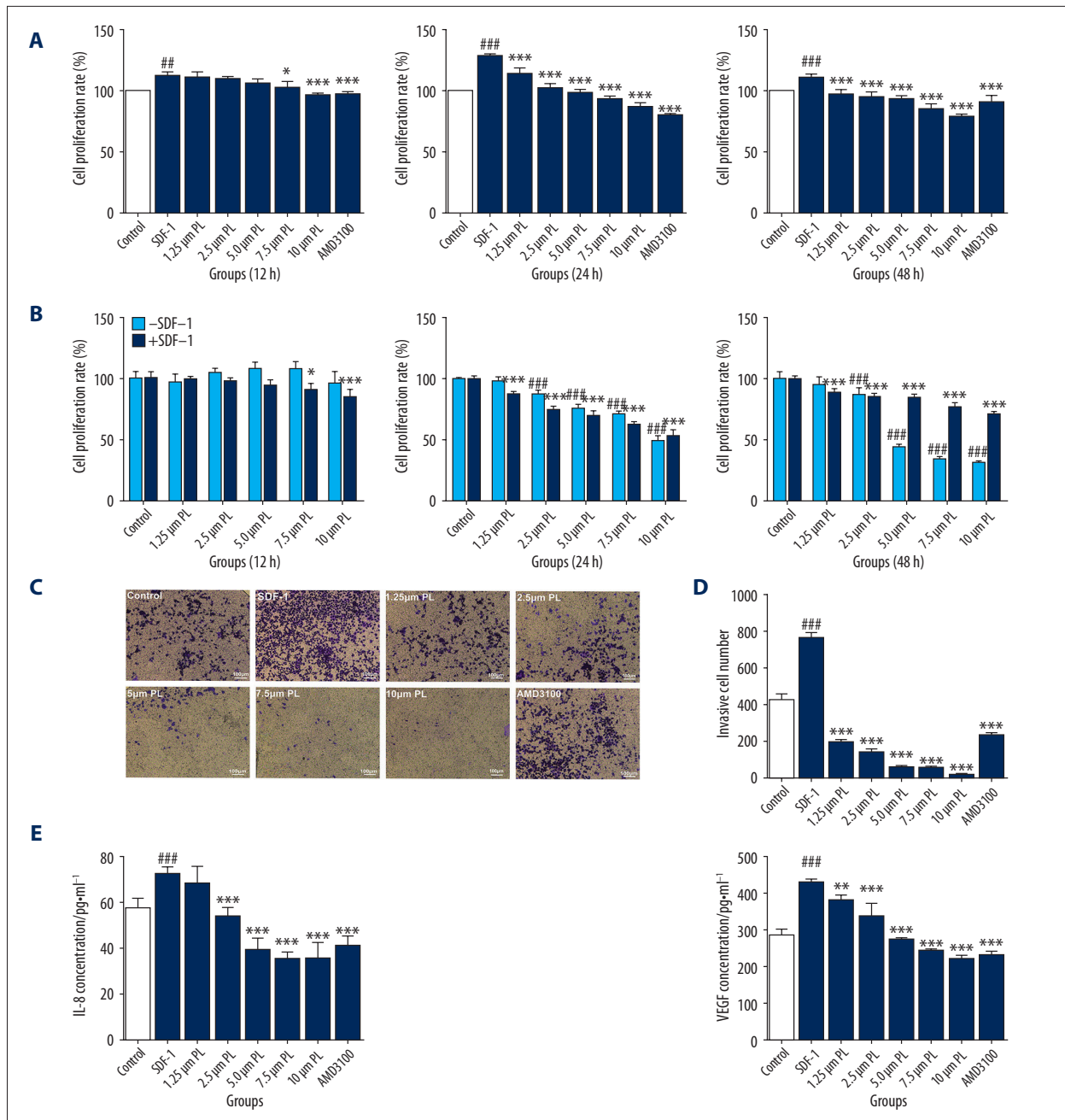


Figure 2. Cell proliferation of SDF-1 (10 ng/ml)-induced SMMC-7721 cells treated with various concentrations of PL (1.25 μm, 2.5 μm, 5 μm, 7.5 μm, and 10 μm) for 12 h, 24 h, or 48 h in a 5% CO₂ incubator at 37°C. AMD3100 (100 ng/ml) was used as the positive control. Each bar represents the mean value ± standard deviation (SD), # P<0.05; ## P<0.01; ### P<0.001, compared to the Control group. * P<0.05; ** P<0.01; *** P<0.001, compared to the SDF-1 group. (A) In the absence of SDF-1, SMMC-7721 cells were treated with different concentrations of PL (1.25 μm, 2.5 μm, 5 μm, 7.5 μm, and 10 μm) for 12 h, 24 h, or 48 h, and their cell proliferation rate was measured. Cells were incubated in a 5% CO₂ incubator at 37°C. P<0.05, ## P<0.01; ### P<0.001; Compared with the control group without SDF-1. * P<0.05; ** P<0.01; *** P<0.001, Compared with the control group with SDF-1 (B). Microscopy of invasion of SDF-1-induced SMMC-7721 cells by different concentrations of PL (1.25 μm, 2.5 μm, 5 μm, 7.5 μm, and 10 μm). AMD3100 (100 ng/ml) was used as the positive control (Scale bar, 100 μm) (C). Numbers of invasive cell SDF-1 induced SMMC-7721 cells by different concentrations of PL (D). Effects of different concentrations of PL (1.25 μm, 2.5 μm, 5 μm, 7.5 μm, and 10 μm) on secretion of IL-8 and VEGF in SMMC-7721 cells. AMD3100 (100 ng/ml) was used as the positive control. Each bar represents the mean value ± standard deviation (SD), # P<0.05; ## P<0.01; ### P<0.001, compared to the Control group. * P<0.05; ** P<0.01; *** P<0.001, compared to the SDF-1 group (E).

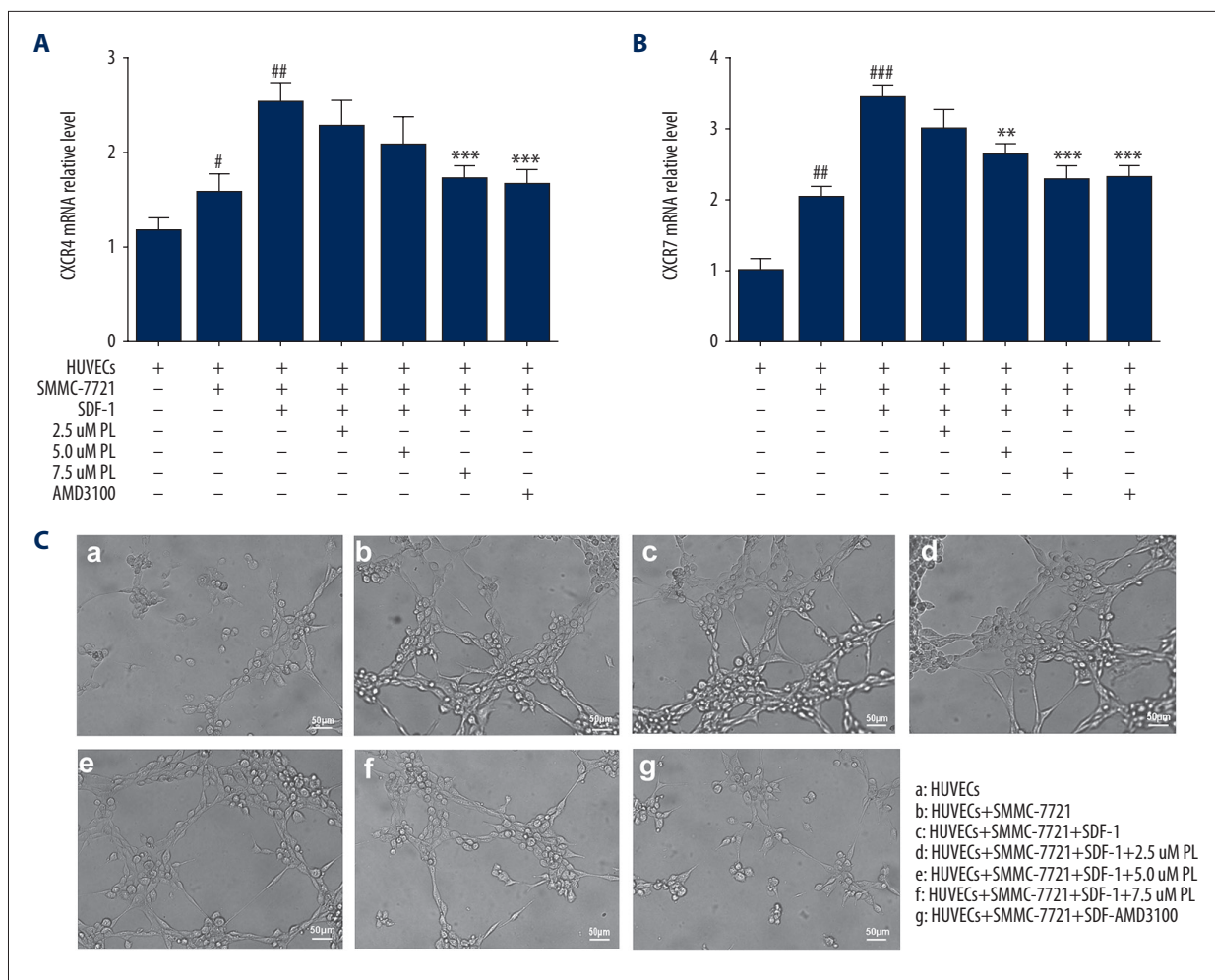


Figure 3. Effect of PL on the mRNA expression of CXCR4 and CXCR7 genes in SMMC-7721 cells co-cultured with HUVECs, grouped as follows: HUVECs only; HUVECs were co-cultured with SMMC-7721 cells; HUVECs were co-cultured with SMMC-7721 induced by SDF-1; the SMMC-7721 cells were treated with 2.5–7.5 μ M PL as indicated; AMD3100 (100 ng/ml) was used as the positive control. After being exposed to the indicated concentrations of PL and AMD3100 for 24 h, the mRNA expression of CXCR4 and CXCR7 were analyzed using quantitative real-time PCR. Each bar represents the mean value \pm standard deviation (SD). * $P < 0.05$; ** $P < 0.01$; *** $P < 0.001$, compared to the HUVEC group. # $P < 0.05$; ## $P < 0.01$; ### $P < 0.001$, compared to the SDF-1 group (A, B). Microscopically co-cultured HUVECs spontaneously form capillary-like structures on Matrigel, particularly SDF-1 induced SMMC-7721 cells. The number and continuity of capillary-like structures in HUVECs were significantly inhibited by 2.5–7.5 μ M PL in a dose-dependent manner (scale bar, 50 μ m) (C).

inhibits angiogenesis-mediated HCC cell proliferation, differentiation, and invasion. The results demonstrated that PL is a potent angiogenesis inhibitor and inhibits multiple steps of angiogenesis, including endothelial cell viability, migration, differentiation into capillary-like structures, and angiogenic factors. The mechanism of PL anti-tumor angiogenesis is achieved by targeting the SDF-1/CXCR4-CXCR7 axis cascade in endothelial HCC cells. Chemokines are small molecular weight proteins (8–13 kDa), and its receptors located on the surface of leukocytes are 7-transmembrane-spanning G protein-coupled proteins, whose $G\alpha 1$ and $G\beta\text{-}\gamma$ subunits dissociate upon receptor binding, leading to activation of downstream pathways [14].

They orchestrate the migration and localization of immune cells in lymph organs and other tissues, exerting the “chemotactic effects” which are necessary for normal immune response *in vivo*. Of all the chemokines and their receptor in HCC, the CXCR subclass accounts for the largest group [3]. SDF-1 promotes proliferation, dissociation, migration, and invasion in a wide variety of tumor cells, including breast cancer cells, pancreatic cancer cells, and HCC cells [16–18]. This study found that SDF-1 significantly stimulated the proliferation and migration of SMMC-7721 cells.

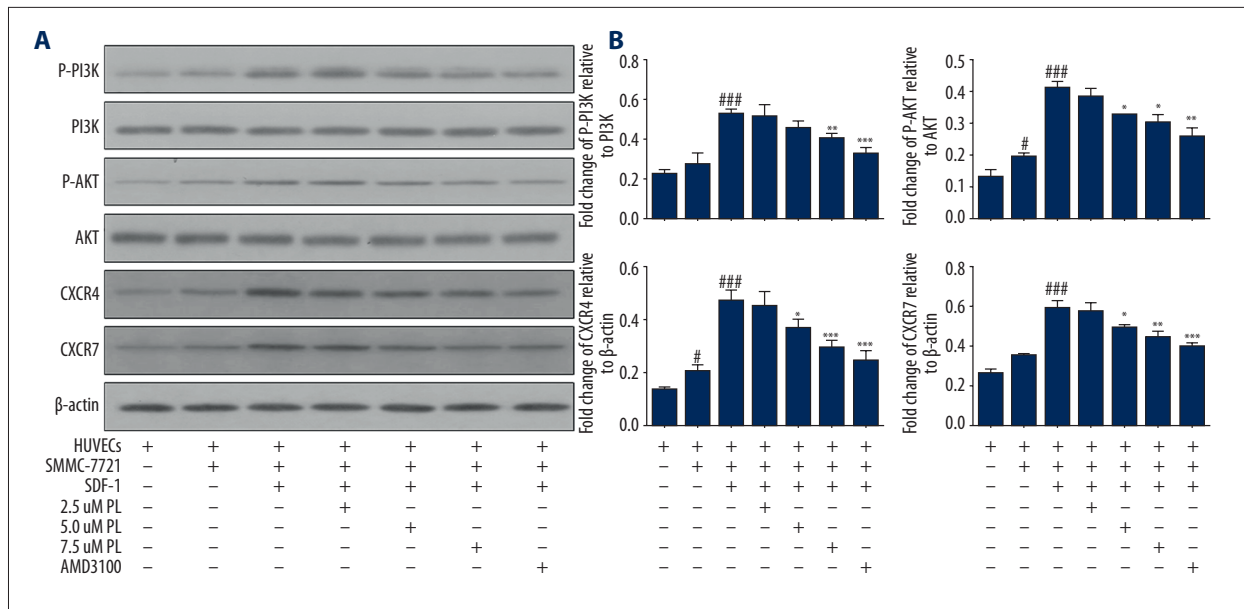


Figure 4. Expression of angiogenesis-related proteins detected by Western blotting after PL treatment, grouped as follows: HUVECs only; HUVECs were co-cultured with SMMC-7721 cells; HUVECs were co-cultured with SMMC-7721 induced by SDF-1; the SMMC-7721 cells were treated with 2.5–7.5 μM PL as indicated; AMD3100 (100 ng/ml) was used as the positive control. The expression of p-Akt, Akt, p-PI3K, PI3K, CXCR4, and CXCR7 proteins in the cells was analyzed by Western blotting using specific antibodies. Akt was used as an internal control for p-Akt, PI3K was used as an internal control for p-PI3K, and β-actin was used as an internal control for CXCR4 and CXCR7. Expression levels of each protein are indicated (A). PL inhibits protein expression. Each bar represents the mean value ± standard deviation (SD). * P<0.05; ** P<0.01; *** P<0.001, compared to the HUVEC group. # P<0.05; ## P<0.01; ### P<0.001, compared to the SDF-1 group (B).

Angiogenesis suppression has become an important focus in the fight against cancer progression. VEGF appears to play key roles in exogenous and endogenous neo-angiogenesis. Binding of VEGF to its receptors leads to dimerization, activation of tyrosine kinase, trans-autophosphorylation, and initiation of extracellular-signal-regulated kinase, Janus kinase, and PI3K/Akt [19–21]. More recently, multifunctional interleukin 8 (IL-8) was found to belong to the superfamily of CXC chemokines, and is potently angiogenic *in vivo* and *in vitro* [22]; the biological effects of IL-8 involve 2 receptors: CXCR1 and CXCR2. IL-8 signaling has been shown to promote transactivation of epidermal growth factor in cancer and vascular endothelial cells [18]. In addition, it induces the phosphorylation of the vascular endothelial growth factor receptor (VEGFR-2) in endothelial cells, regulating the permeability of the endothelial barrier [23]. Our results indicated that SDF-1-induced and HCC cell-derived SDF-1 release VEGF/IL-8, which in turn supports tumor progression through angiogenesis. In contrast, VEGF is generated by tumor cells but can be mediated by SDF-1 [15]. Plumbagin can eliminate the formation of tumor vasculature by reducing angiogenic cytokine-induced and SDF-1-induced endothelial cell proliferation. *In vitro* angiogenic cytokine-induced SMMC-7721 cells effectively reduce the ability to proliferate, invade, and form capillary-like structures after PL treatment.

An emerging chemokine target for cancer therapy is SDF-1, which binds and initiates signaling through its cognate receptors, CXCR4 and CXCR7 [24,25]. CXCR4 belongs to the family of 7-transmembrane G protein-coupled receptors (GPCR), but CXCR7 is involved in differentiation. Much less know about the classical GPCR mobilization of Ca²⁺, which we did not observe, and its biological effect occurs via the β-arrestin-2 pathway. CXCR7 was identified to be an SDF-1 receptor with a 10-fold-higher binding affinity toward CXCL12 than CXCR4. Similar to CXCR4, high CXCR7 expression has been found in hepatoma cell lines and metastatic HCC samples [12,26–28]. In the present study, we show for the first time that plumbagin obviously suppresses the levels of CXCR4 and (especially) CXCR7, when the SMMC-7721 (SDF-1-induced or not) were co-cultured with HUVEC cells.

CXCR4 and CXCR7 may have the ability to form heterodimers. CXCR4/CXCR7 heterodimer led to constitutive recruitment of β-actin to form the CXCR4/CXCR7/β-actin complex, which potentiates the SDF-1-mediated downstream pathways. Several recent reports suggest that PI3K/Akt signaling also induces angiogenesis in various tumors. PI3Ks play a pivotal role in diverse cellular processes, including proliferation, differentiation, migration, trafficking, apoptosis, and glucose homeostasis [29,30]. AMD3100 is a CXCR4 antagonist against chemokines

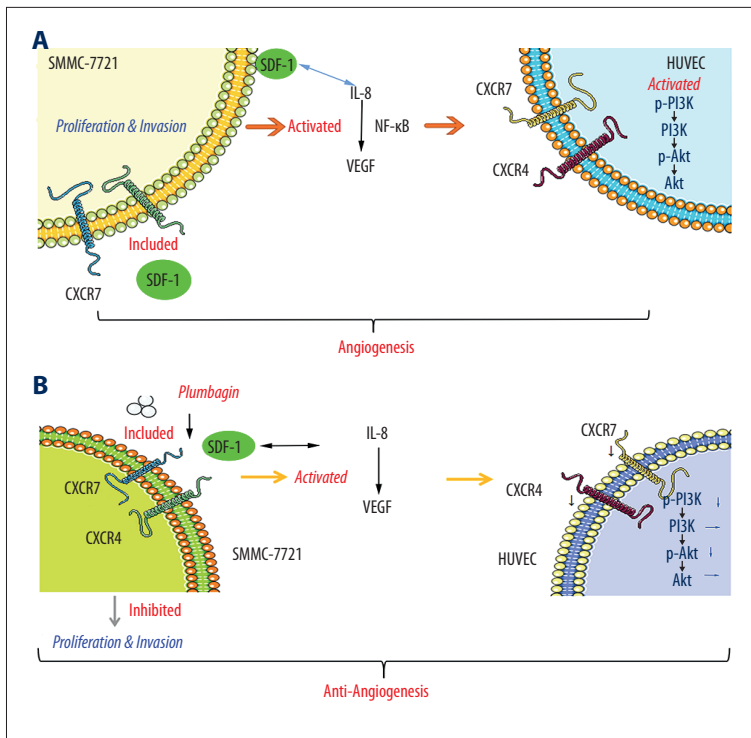


Figure 5. SDF-1 induces angiogenesis-related signaling pathways in HUVECs co-cultured with SMMC-7721 hepatocellular carcinoma cells (A). PL inhibits the angiogenic SDF-1/CXCR4-CXCR7 axis activity of HUVECs co-cultured with SMMC-7721 hepatoma cells, downregulates the mechanism of PI3K/Akt pathway, and improves the microenvironment of hepatocellular carcinoma (B).

and is very common in cancer therapy [31]. SMMC-7721 cells were co-cultured with HUVEC cells that had hepatocarcinoma angiogenesis, and treatment with AMD3100 significantly reduced the expression of PI3K/Akt in SMMC-7721 cells and endothelial cells, in a time-dependent manner. In addition, PI treatment also inhibited the expression of PI3K and Akt by up-regulating the phosphorylation levels of PI3K and Akt.

Conclusions

Our results indicate that SDF-1 can directly promote the proliferation and invasion of SMMC-7721 cells and directly or indirectly increase the concentration of VEGF and IL-8. In contrast, SDF-1 induces the release of VEGF from HCC cells, which activates the transcription factor NF-κB through autocrine activation of the receptor VEGFR-2 in endothelial cells, thereby producing IL-8 and exerting positive feedback control for SDF-1 [14]. The mechanism is as shown in Figure 5A. In addition, SDF-1 can activate intracellular signals, such as phosphorylation of PI3K/Akt, alone or in combination with the

CXCR4 or CXCR7 axis. Several studies have indicated that the SDF-1/CXCR7 axis regulates the levels of extracellular SDF-1 and the SDF-1/CXCR4 axis to regulate downstream signaling [27,32–34]. However, PL inhibits the proliferation and invasion of SMMC-7721 cells induced by SDF-1, and decreases the concentration of VEGF and IL-8 induced by SDF-1 in SMMC-7721 cells. In addition, in SMMC-7721 cells co-cultured with HUVECs, we found that PL can significantly inhibit the angiogenesis of SMMC-7721 and HUVECs co-cultured cells induced by SDF-1, and downregulate the mRNA expression of CXCR4 and CXCR7 (Figure 5B).

Conclusions

The effect of PL on the SDF-1-CXCR4/CXCR7 axis has become an attractive target for inhibiting angiogenesis in hepatoma cells. Our study provides more evidence for the clinical application of PL, which belongs to traditional medicine, in modern cancer treatment.

References:

- Chen W, Zheng R, Zhang S et al: Report of cancer incidence and mortality in china, 2010. *China Cancer*, 2013; 40: 5
- Mercedes F, David S, Jordi B et al: Angiogenesis in liver disease. *J Hepatol*, 2009; 50: 604–20
- Liang CM, Chen L, Hu H et al: Chemokines and their receptors play important roles in the development of hepatocellular carcinoma. *World J Hepatol*, 2015; 7: 1390–402
- Sumsakul W, Plengsuriyakarn T, Na-Bangchang K: Pharmacokinetics, toxicity, and cytochrome p450 modulatory activity of plumbagin. *BMC Pharmacol Toxicol*, 2016; 17: 50
- Wei YF, Jing-Qiang LI, Zhang ZW et al: [Effects of plumbagin on cell cycle of human hepatic stellate cells stimulated by leptin and its related protein expression.] *Chinese Traditional & Herbal Drugs*, 2012; 43: 1776–780 [in Chinese]

6. Wei YF, Huang RB: [Effects of plumbagin on apoptosis and expression of apoptosis-related proteins in human hepatic stellate cells.] *World Chinese Journal of Digestology*, 2011; 19: 349–54 [in Chinese]
7. Shieh JM, Chiang TW: Plumbagin inhibits tpa-induced mmp-2 and u-pa expressions by reducing binding activities of nf-kappab and ap-1 via erk signaling pathway in a549 human lung cancer cells. *Mol Cell Biochem*, 2010; 335: 181–93
8. Tian L, Yin D, Ren Y et al: Plumbagin induces apoptosis via the p53 pathway and generation of reactive oxygen species in human osteosarcoma cells. *Mol Med Rep*, 2012; 5: 126–32
9. Manu KA, Shanmugam MK, Rajendran P et al: Plumbagin inhibits invasion and migration of breast and gastric cancer cells by downregulating the expression of chemokine receptor cxcr4. *Mol Cancer*, 2011; 10: 107
10. Wei YF, Yang Q, Zhang Y et al: Plumbagin restrains hepatocellular carcinoma angiogenesis by suppressing the migration and invasion of tumor-derived vascular endothelial cells. *Oncotarget*, 2017; 8: 15230–41
11. Lin Y, Chen Y, Wang S et al: Plumbagin induces autophagy and apoptosis of smmc-7721 cells *in vitro* and *in vivo*. *J Cell Biochem*, 2019; 120(6): 9820–30
12. Liepelt A, Tacke F: Stromal cell-derived factor-1 (sdf-1) as a target in liver diseases. *Am J Physiol Gastrointest Liver Physiol*, 2016; 311(2): G203–9
13. Chen Y, Teng F, Wang G, Nie Z: Overexpression of cxcr7 induces angiogenic capacity of human hepatocellular carcinoma cells via the akt signaling pathway. *Oncol Rep*, 2016; 36: 2275
14. Ehling J, Tacke F: Role of chemokine pathways in hepatobiliary cancer. *Cancer Lett*, 2016; 379: 173–83
15. Zheng K, Li HY, Su XL et al: Chemokine receptor cxcr7 regulates the invasion, angiogenesis and tumor growth of human hepatocellular carcinoma cells. *J Exp Clin Cancer Res*, 2010; 29: 31
16. Ma DM, Luo DX, Zhang J: Sdf-1/cxcr7 axis regulates the proliferation, invasion, adhesion, and angiogenesis of gastric cancer cells. *World J Surg Oncol*, 2016; 14: 256
17. Huang M, Li Y, Zhang H, Nan F: Breast cancer stromal fibroblasts promote the generation of cd44+ cd24– cells through sdf-1/cxcr4 interaction. *J Exp Clin Cancer Res*, 2010; 29: 80
18. Schraufstatter IU, Chung J, Burger M: IL-8 activates endothelial cell cxcr1 and cxcr2 through rho and rac signaling pathways. *Am J Physiol Lung Cell Mol Physiol*, 2001; 280: 1094–103
19. Li Z, Wang B, Tang L et al: Quinazoline derivative compound (11d) as a novel angiogenesis inhibitor inhibiting vegfr2 and blocking vegfr2-mediated akt/mTOR/p70s6k signaling pathway. *Iran J Basic Med Sci*, 2016; 19: 411–16
20. Zhang L, Wang JN, Kong X et al: Vegf is essential for the growth and migration of human hepatocellular carcinoma cells. *Mol Biol Rep*, 2012; 39: 5085–93
21. Peng-Yuan Z, Jun S, Xiao-Dong Z et al: Prognostic roles of cross-talk between peritumoral hepatocytes and stromal cells in hepatocellular carcinoma involving peritumoral vegf-c, vegfr-1 and vegfr-3. *PLoS One*, 2013; 8: e64598
22. Kubo F, Ueno S, Hiwatashi K et al: Interleukin 8 in human hepatocellular carcinoma correlates with cancer cell invasion of vessels but not with tumor angiogenesis. *Ann Surg Oncol*, 2005; 12: 800–7
23. Waugh DJJ, Catherine W: The interleukin-8 pathway in cancer. *Clin Cancer Res*, 2008; 14: 6735
24. Rath D, Chatterjee M, Holtkamp A et al: Evidence of an interaction between tgf-β1 and the sdf-1/cxcr4/cxcr7 axis in human platelets. *Thromb Res*, 2016; 144: 79–84
25. Qiang L, Aijun Z, Changbo T et al: The role of sdf-1-cxcr4/cxcr7 axis in biological behaviors of adipose tissue-derived mesenchymal stem cells *in vitro*. *Biochem Biophys Res Commun*, 2013; 441: 675–80
26. Dan G, Duda Kozin SV, Kirkpatrick ND et al: Cxcl12 (sdf1alpha)-cxcr4/cxcr7 pathway inhibition: An emerging sensitizer for anticancer therapies? *Clin Cancer Res*, 2011; 17: 2074
27. Lin L, Han MM, Wang F et al: Cxcr7 stimulates mapk signaling to regulate hepatocellular carcinoma progression. *Cell Death Dis*, 2014; 5: e1488
28. Xu D, Li R, Wu J et al: Drug design targeting the cxcr4/cxcr7/cxcl12 pathway. *Curr Top Med Chem*, 2016; 16: 1441–51
29. Amanda P, Nikolaos A, Maria V et al: Pathways and targets in hepatocellular carcinoma. *Expert Rev Anticancer Ther*, 2012; 12: 1347–57
30. Montella L, Palmieri G, Addeo R, Prete SD: Hepatocellular carcinoma: Will novel targeted drugs really impact the next future? *World J Gastroenterol*, 2016; 22: 6114–26
31. Cashen AF, Bruno N, John DP: Amd3100: Cxcr4 antagonist and rapid stem cell-mobilizing agent. *Future Oncol*, 2007; 3: 19–27
32. Ismael G, Riveiro ME, Valerie P et al: Insights on the cxcl12-cxcr4 axis in hepatocellular carcinoma carcinogenesis. *Am J Transl Res*, 2014; 6: 340–52
33. Ziegler ME, Hatch MMS, Wu N et al: Mtorc2 mediates cxcl12-induced angiogenesis. *Angiogenesis*, 2016; 19: 359–71
34. Yamada K, Maishi N, Akiyama K et al: Cxcl12-cxcr7 axis is important for tumor endothelial cell angiogenic property. *Int J Cancer*, 2015; 137: 2825–36